BOREAL ENVIRONMENT RESEARCH 19: 115–126
ISSN 1239-6095 (print) ISSN 1797-2469 (online)
© 2014
Helsinki 25 April 2014

Empiric equations of coagulation sink of fine nanoparticles on background aerosol optimized for boreal zone

Hannes Tammet[1)] and Markku Kulmala[2)]

[1)] *Institute of Physics, University of Tartu, Ülikooli 18, EE-50090 Tartu, Estonia*
[2)] *Division of Atmospheric Sciences, Department of Physics, P.O. Box 64, FI-00014 University of Helsinki, Finland*

Received 17 Dec. 2013, final version received 2 May 2013, accepted 2 May 2013

Tammet, H. & Kulmala, M. 2014: Empiric equations of coagulation sink of fine nanoparticles on background aerosol optimized for boreal zone. *Boreal Env. Res.* 19: 115–126.

Fundamental models of aerosol nanoparticle coagulation sink in the atmosphere are sophisticated and require detailed knowledge about the size distribution of background aerosol particles. Here, we present empiric equations which help to make quantitative relations graspable and support quick and rough estimation of the coagulation sink according to background aerosol particle concentration and vice versa when browsing limited data. Accuracy of an empiric equation is described by a deviation between the results obtained according to two methods: fundamental models and empiric equations. Optimizing empiric equations is discussed considering a set of aerosol size distributions measured at the SMEAR II station, Finland, during years 2008–2010. Fundamental models include the particle-particle coagulation model by Dahneke and the air ion attachment model by Hoppel and Frick. Small air ions are considered a special kind of nanoparticles. The background aerosol is characterized with a power-weighted integral concentration in a restricted range of particle diameters. The power exponent and borders of the diameter range are adjusted when optimizing the equation. Nanoparticles are represented with a power function of the diameter or with the electric mobility. Compromises between the simplicity of the equation and the accuracy of the approximation are considered and different versions of empiric equations are proposed.

Introduction

Understanding of climate changes requires knowledge about processes controlling the Earth's cloud cover including the formation of new particles in atmospheric air and their growth up to the size of cloud condensation nuclei. The growth is controlled by the condensation of gaseous components on the nanometer size seeds of particles and by the scavenging of these seeds due to coagulation with preexisting coarse particles of a background aerosol (Kulmala 2003, Kulmala *et al*. 2004, Westervelt *et al*. 2012). New particle formation and growth are sensitive to the variation of the coagulation sink of the finest nanoparticles (Kerminen and Kulmala 2002, Kulmala *et al*. 2012, Kulmala *et al*. 2013).

If the distribution of aerosol particles according to their size is known then the coagulation sink can be calculated according to a fundamental model as an integral over the product of the coagulation coefficient and the distribu-

Editor in charge of this article: Hannele Korhonen

tion function. An ordinary computer can examine a large dataset during a few seconds, and replacing a fundamental model with a simple empiric equation does not have considerable effect on data processing. This raises a question why empiric equations are needed. Empiric equations have different applications. In some situations they help to make quantitative relations comprehensible. For example, Lehtinen *et al*. (2007) showed that coagulation sink depends on the diameters of nanoparticles approximately according to the power law with an empiric exponent of about –1.6. This result has perceptive value and resolves the earlier theoretical discussion where the value of the power exponent was usually assumed to be –2 or –1. Another application is quick and rough estimation of the coagulation sink according to the concentration of background aerosol particles and vice versa when browsing limited data. The detailed size distributions of background aerosol particles are measured only in well-equipped stations of atmospheric aerosol research (Manninen *et al*. 2010) and are usually not openly accessible. Journal publications may include only few examples of detailed distribution function. The integral parameters like number concentrations of particles in specified size ranges are more widely available. Here, a proper empiric equation can be useful as a practical tool. Additionally, the empiric equations may have applications in approximate mathematical models of nanoparticle and air ion dynamics.

Theoretical estimates and statistical characteristics of coagulation sink in boreal atmospheric air have been analyzed in earlier studies by Dal Maso *et al*. (2002, 2005) and by Lehtinen *et al*. (2007) using the data recorded during 1996–2003 at the SMEAR II station in Hyytiälä, Finland (Hari and Kulmala 2005). The present study is based on the measurements made at the same station during three years (2008–2010) using improved instrumentation and methods. The shapes of background aerosol size distributions in European unpolluted low altitude stations are relatively similar with the exception of one seashore station (Asmi *et al*. 2011). The main differences between stations can be found in levels of concentration. Empiric equations which do not have pretensions of high accuracy may appear representative for a wide geographic zone. The quality criteria for an empiric equation are comprehensibility, convenience in applications and good match of results with fundamental models. Our choices for reference fundamental models are the model of coagulation in transition regime by Dahneke (1983) recommended by Gopalakrishnan and Hogan (2011), and the Hoppel-Frick model of the attachment of air ions to aerosol particles (Hoppel and Frick 1990).

Conventions

The chemical composition and internal structure of particles are not discussed in the present paper and all particles are considered spheres of definite diameter. The size range of fine nanoparticles is limited to the diameter of 10 nm, and particles with diameters larger than 10 nm are considered background aerosol particles. Small ions are a special kind of electrically charged nanoparticles with a typical diameter of 0.7–0.8 nm. We assume that the concentration of nanoparticles is low and their sink is caused by coagulation with background particles. This means that the nanoparticle-nanoparticle coagulation is neglected. The sink of nanoparticles S is measured in s^{-1} and defined as the relative intensity of loss in an imaginary situation when there is no supply of particles

$$S = -\frac{1}{N}\frac{dN}{dt}. \quad (1)$$

Here N is the concentration of particles in the investigated size category. The sink of nanoparticles depends on the size and electric charge of nanoparticles and on the size and charge distributions of the background aerosol particles. The distribution of electric charges of aerosol particles in natural atmospheric air does not usually greatly deviate from the thermodynamic equilibrium distribution and the probability to have more than one elementary charge on a nanoparticle is negligible. Thus the nanoparticles are considered neutral or singly charged spheres.

Particle size distribution is described by the function $n(d_p) = dN/dd_p$, where N is the number concentration of the particles whose diameter does not exceed d_p. When plotting the distribu-

tions in a wide range of diameters, the function $dN/d[\log(d_p)] = \ln(10) d_p n(d_p)$ is often used. The category of particles can be accented by replacing the universal index 'p' with a specified index: 'n' marks the nanoparticles, 'b' the background aerosol particles, 0 the neutral particles, 1 the singly charged particles and 'q' the particles with q elementary charges. The sink can be expressed separately for neutral particles or charged particles. The full sink of charge-specified particles includes a coagulation component and a charging or neutralization component. The coagulation sink includes only the coagulation component.

Background particles in the humid natural air contain some amount of water. We assume that part of the water is lost in the measuring process and the size distributions are recorded for slightly shrunken particles. The diameter of background particles in an analyzer (d_b) is called the measured diameter and indicated on the horizontal axis when plotting the diagrams of size distributions. However, the sink of nanoparticles is to be calculated considering the hygroscopic growth of background particles. Corresponding natural diameter of a particle in the atmosphere is marked with the index 'h' and it can slightly exceed the measured diameter: $d_h > d_b$. The data obtained from published measurements correspond, as a rule, to the diameter d_b. Thus the diameter d_b is used as an argument in empiric equations, which should represent the correlation between the coagulation sink and the measurements of aerosol parameters.

The power-weighted integral concentration of background aerosol particles in a size range (d_1, d_2)

$$N_{k,d_1-d_2} = \int_{d_1}^{d_2} \left[\frac{d_b}{1\ \mathrm{nm}}\right]^k n_b(d_b)\, dd_b \qquad (2)$$

has the unit of cm^{-3} independent of the power exponent k. The number concentration of background particles in a size range (d_1, d_2) is

$$N_{d_1-d_2} = N_{0,d_1-d_2} = \int_{d_1}^{d_2} n_b(d_b)\, dd_b. \qquad (3)$$

A widely used range-specific number concentration N_{50-500} includes background particles with diameters from 50 to 500 nm. The boundaries of the background particle diameters d_1 and d_2 are shown in the index as expressed in nanometers. The dimensionless numeric value of the nanoparticle diameter as measured in nanometers is denoted $d_{n/nm} = d_n/1\ \mathrm{nm}$. This quantity can be raised to a fractional power without dimension problems.

Reference data

Data used in the present study were acquired during three years (2008–2010) at the SMEAR II station (Station for Measuring Forest Ecosystem–Atmosphere Relations) located in Hyytiälä, Finland (61°31´N, 24°17´E, 181 m a.s.l., 220 km NW from Helsinki), and run by the University of Helsinki (Hari and Kulmala 2005). The station provided data for the networks of European Supersites for Atmospheric Aerosol Research (EUSAAR, *see* http://www.eusaar.net/upload/SMEAR2.pdf) and EMEP/GAW joint super sites (Asmi *et al*. 2011). The air quality in Hyytiälä represents typical regional background conditions in southern boreal zone of Europe. The instruments are located in a cottage within a Scots pine stand. Conditions of measurements were the same as described by Virkkula *et al*. (2011). Distribution of particles according to the diameter was measured using the Differential Mobility Particle Sizers (DMPS) with Hauke-type DMAs and the Aerodynamic Particle Sizer (APS) TSI model 3321. The DMPS data of the distribution function $dN/d[\log(d_p)]$ is given at 38 geometric diameters in the range of 3–980 nm and the APS data at 52 aerodynamic diameters in the range of 520 nm–19.8 μm. During data preparation, the two datasets were merged by converting the aerodynamic diameters to geometric diameters by the factor of 0.82, following the argumentation by Virkkula *et al*. (2011). Exactness of the conversion is not critical in the present study because most of the nanoparticle sink is caused by background particles in the size range of DMPS measurements.

Data was originally recorded with the time interval of 10 min and presented with 1107 diurnal files for DMPS measurements and 1051 diurnal files for APS measurements. About 90% of available time is covered with both DMPS and APS measurements. The reference dataset was compiled in the following way: First, the hourly

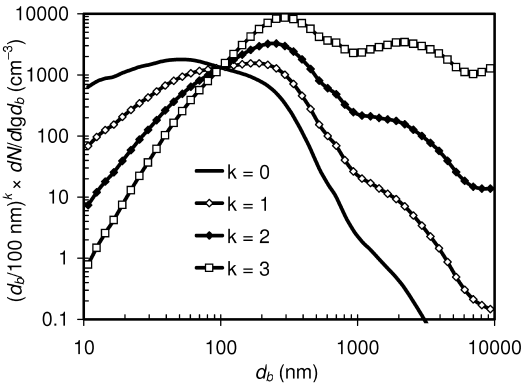

Fig. 1. Mean size distributions $(d_b/100\ \mathrm{nm})^k \times dN/d\lg d$ as recorded in Hyytiälä during the three years (2008–2010). Markers are depicted according to 1/16-decade fractions.

averages were calculated, including only the hours that had at least 3 datapoints. Next, the distributions of particles according to the measured diameter were converted into the logarithmically uniform grid with 16 size intervals in a diameter decade, where the geometric centers of the intervals from 2.94 nm to 14.3 μm are $d_{bi} = 10^{(i+6.5)/16}$, $i = 1, ..., 60$ (only the subset $i = 10, ..., 57$ is used in the present study). The diameter grid was chosen to match the original grid of most of the instrument recordings. The simultaneous DMPS and APS data were merged so that the overlapping size range of 500–1000 nm was filled with the weighted averages

$$n(d_b) = [(1000\ \mathrm{nm} - d_b)n_{\mathrm{DMPS}}(d_b) + (d_b - 500\ \mathrm{nm})n_{\mathrm{APS}}(d_b)]/500\ \mathrm{nm}. \quad (4)$$

Here $n_{\mathrm{DMPS}}(d_b)$ and $n_{\mathrm{APS}}(d_b)$ are the distribution functions from the DMPS and APS instruments.

Table 1. Mean values of GF_{90} according to Fors *et al.* (2011), the approximation (Eq. 5), and ratio of humid and measured diameters estimated according to Eq. 6.

d_{dry} (nm)	GF_{90} (Fors 2011)	Approx. GF_{90}	Estimated d_h/d_b
35	1.30	1.29	1.14
50	1.32	1.32	1.16
75	1.35	1.36	1.18
110	1.41	1.40	1.20
165	1.47	1.44	1.22
265	1.51	1.48	1.24

Finally, the data were analyzed with the aim of detecting possible defects. During this step about 7% of records were eliminated because recognizable distortions were detected, mostly lack of data in some size segment. The final dataset includes 21 682 hours of data, which covers 82.5% of possible hours during the considered period. Mean distributions of number concentration and power-weighted concentrations are plotted in a logarithmic diagram (Fig. 1).

The coagulation sink depends on the size of the background aerosol particles in natural air where they contain some water. The reference data are tabulated according to particle measured diameter d_b and do not include the information necessary for exact determination of the ratio of the natural diameter d_h to the measured diameter d_b. The standard hygroscopic growth factor GF_{90} corresponds to the change in relative humidity from a very low value to 90%. The relative humidity inside the instruments is only partially reduced and the humidity of outdoor air is usually less than 90%. Thus the ratio $d_h/d_b < GF_{90}$. We accept a rough approximation assuming 50% of the full hygroscopic growth

$$d_h = [1 + (GF_{90} - 1)/2]d_b. \quad (5)$$

Ehn *et al.* (2007) investigated the factor GF_{90} for particles up to dry diameter of 50 nm in Hyytiälä and found that GF_{90} increases with the particle size and has a distinct diurnal variation around the value of about 1.25 in case of the dry diameter of 50 nm. The sink of nanoparticles is caused mostly by particles larger than 100 nm in diameter. Adam *et al.* (2012) found mean GF_{90} of about 1.32 for 165 nm particles in Italy. Fors *et al.* (2011) recorded GF_{90} in the Swedish rural station of Vavihill during 27 months in 2008–2010 and found the mean diurnal variation of GF_{90} to be between 1.30 and 1.33 for the dry diameter of 50 nm and between 1.45 and 1.48 for the dry diameter of 165 nm (Table 1), while the scattering of values from hour to hour was low and characterized with a standard deviation of about 0.1. We will use an approximation

$$GF_{90} \approx 1.5 - 0.3\exp(-d_b/100\ \mathrm{nm}) \quad (6)$$

based on results by Fors *et al.* (2011).

Sink of neutral nanoparticles

The size distribution of background aerosol particles is originally presented according to the measured diameter d_b. Coagulation sink of neutral nanoparticles of diameter d_n on background aerosol particles depends on the natural diameters d_h and can be calculated as

$$\begin{aligned} S(d_n) &= \int \beta_0(d_n, d_h) n_h(d_h)\, dd_h \\ &= \int \beta_0(d_n, d_h) n_b(d_b)\, dd_b \end{aligned}, \quad (7)$$

where d_h and d_b are related according to Eqs. 5 and 6 and $\beta_0(d_n,d_h)$ is the mutual coagulation coefficient for two neutral particles. In our earlier work (Tammet and Kulmala 2005), coagulation coefficients were calculated according to Sahni interpolation between the free molecule regime and the continuum regime as recommended by Fuchs and Sutugin (1971). Gopalakrishnan and Hogan (2011) confirmed the earlier conclusion by Otto *et al*. (1999) that a better compromise between exactness and computational simplicity is offered by the interpolation by Dahneke:

$$\left.\begin{aligned} \beta_{fm} &= (d_n + d_h)^2 \sqrt{\frac{\pi kT(m_n + m_h)}{2 m_n m_h}} \\ \beta_{co} &= 2\pi kT(B_n + B_h)(d_n + d_h) \\ \kappa &= \frac{\beta_{co}}{\beta_{fm}} \\ \beta_0 &= \beta_{co} \frac{2+\kappa}{2+2\kappa+\kappa^2} \end{aligned}\right\}, \quad (8)$$

where β_{fm} and β_{co} are the limits of coagulation coefficient for the free molecule regime and the continuum regime, k is the Boltzmann constant, T is the absolute temperature, m_n and m_h are the masses of the nanoparticle and the background particle, B_n and B_h are the mechanical mobilities of these particles, and κ is the Dahneke's analogue of the Knudsen number. Electrical and mechanical mobilities are calculated according to Tammet (1995, 2012).

We assume in the following discussion that the background particles may be electrically charged and that the distribution according to the charge corresponds to the thermodynamic equilibrium. Charge of a background particle polarizes the neutral nanoparticle and may enhance the coagulation. Effect of polarization can be theoretically estimated using the kinetic theory and the $(\infty - 4)$ potential model, which considers a nanoparticle a hard sphere with an elementary charge located in the centre of the sphere. Numeric calculation using the approximation of the collision integral according to Tammet (1995) showed that the polarization can enhance the coagulation of neutral nanoparticles with equilibrium-charged background aerosol particles by up to 0.02% when assuming the mean size distribution in the reference set of background aerosol measurements. Thus the nanoparticle polarization is neglected in the following discussion and the coagulation coefficients for neutral nanoparticles are calculated according to Dahneke interpolation without additional corrections.

The distribution function of the sink as a function of the particle diameter equals to the product of the coagulation coefficient and the distribution function of background particles, and the coagulation coefficient is calculated considering corresponding natural diameters of the background particles:

$$\frac{dS}{dd_b}(d_n, d_b) = \beta_0(d_n, d_h) n_b(d_b). \quad (9)$$

Mean distributions of the sink of different sized nanoparticles on the reference set of background aerosol measurements is illustrated with a diagram (Fig. 2) in the similar way as the distribution of number concentration. Some size regions of background aerosol particles have important contribution to the sink and some play a minor role (Table 2). About 90% of the coagulation sink of nanoparticles is caused by background aerosol particles with a measured diameter of 50–500 nm.

Lehtinen *et al*. (2007) showed that the sink of fine nanoparticles is approximately proportional to $d_{n/nm}^{-m}$, where the exponent m is typically 1.6–1.7. The present calculations confirm this conclusion. If the sink is expected to be proportional to $d_{n/nm}^{-m}$, then the ratio S_2/S_1 for the diameters of d_1 and d_2 is $(d_1/d_2)^m$ and mean m for an interval (d_1,d_2) can be estimated as $m = \ln(S_2/S_1)/\ln(d_1/d_2)$ (Lehtinen *et al*. 2007). Corresponding estimates

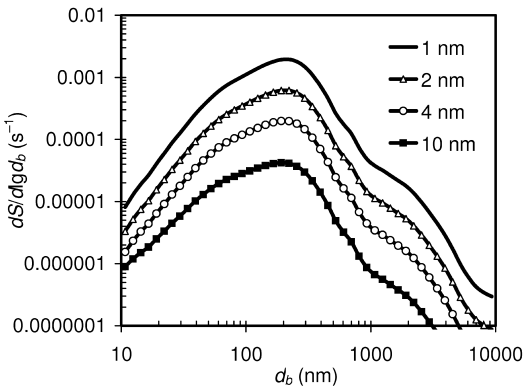

Fig. 2. Mean distribution of the sink of neutral nanoparticles with the diameters of 1, 2, 4 and 10 nm on the reference set of background aerosol measurements. The sink is calculated considering the natural diameters of background particles but presented in the scale of measured diameters.

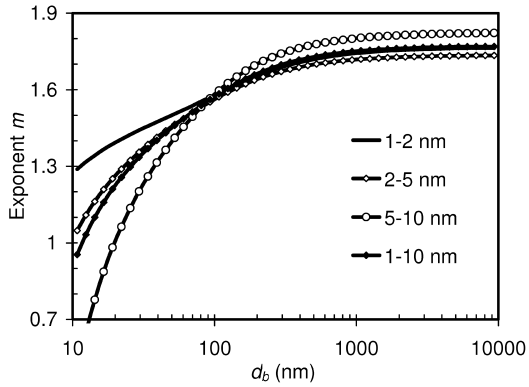

Fig. 3. Mean power law exponent $m = \ln(S_2/S_1)/\ln(d_1/d_2)$ for different intervals of nanoparticle diameter as a function of the diameter of background particles (assumed here monodisperse).

of m for monodisperse background aerosol particles are illustrated with a diagram (Fig. 3). The sink on the polydisperse background aerosol is dominated by particles with the diameter of 100–300 nm (Fig. 3) where the power exponents are close to m = 1.6–1.7 (Fig. 3).

The sink is positively correlated with the concentration of background aerosol particles in any specified size range. The corresponding empiric equation is

$$S \approx a{d_{\mathrm{n/m}}}^{-m} N_{k,d_1-d_2}, \qquad (10)$$

where the power-weighted concentration of background particles is calculated according to Eq. 2. The background particle diameter limits d_1 and d_2 are chosen 50–500 nm or 10–10000 nm as usual in practice of aerosol measurements. Three parameters of empiric equation a, m, and k are to be evaluated according to the criterion of minimum of the geometric standard deviation (GSD) between the estimates of the sink according to Eq. 10 and the reference values calculated according to Eqs. 7 and 8. In case of small variation, GSD is replaced with the relative standard deviation RSD = $\sigma/\mu \approx$ GSD – 1, where μ is the arithmetic mean of the sink and σ is the standard deviation of the difference between the empiric estimates and the reference values of the sink.

The numeric experiments were made considering the full set of 21 682 background aerosol distributions while the values of $d_{\mathrm{n/nm}}$ were randomly chosen from the set of integers 1–10, corresponding to d_{n} values 1 – 10 nm. The quality of approximation depends on the range of the background particle diameters under consideration and the two exponents m and k. The full size range of 10 nm–10 μm allows achieving a minimum value of RSD of about 4.5% through the reference set of hourly average distributions in Hyytiälä (Fig. 4). The corresponding approximation

Table 2. Percentages of the coagulation sink of different sized nanoparticles caused by different classes of background particles in case of the mean size distribution of reference aerosol. d_{n} and d_{b} denote the nanoparticle and background particle diameters.

	$d_{\mathrm{b}} < 20$ nm	$d_{\mathrm{b}} < 50$ nm	$d_{\mathrm{b}} = 20$–500 nm	$d_{\mathrm{b}} = 50$–500 nm	$d_{\mathrm{b}} > 500$ nm
$d_{\mathrm{n}} = 1$ nm	0.5	5.5	95.4	90.4	4.1
$d_{\mathrm{n}} = 2$ nm	0.6	6.2	95.6	90.0	3.8
$d_{\mathrm{n}} = 4$ nm	0.8	7.2	95.7	89.3	3.5
$d_{\mathrm{n}} = 10$ nm	1.5	10.1	95.5	86.9	3.0

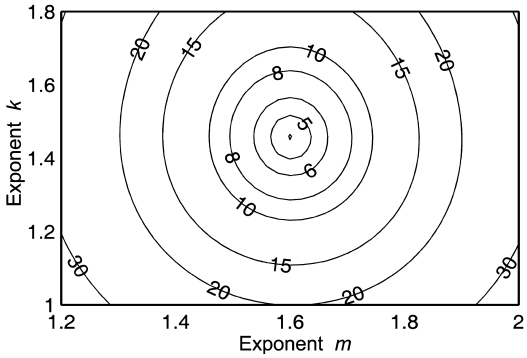

Fig. 4. Dependence of the quality of approximation (measured as relative standard deviation in percents) on the parameters m and k of the equation $S \approx a d_{n/nm}^{-m} N_{k,10-10000}$.

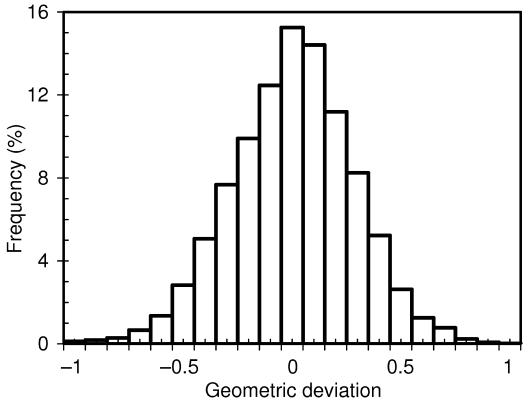

Fig. 5. Distribution of geometric deviation $\ln(S_{approximate}/S_{reference})$ between the empiric Eq. 12 and the reference model (Eqs. 7 and 8).

$$S \approx (1.03 \times 10^{-9}\ \mathrm{cm^3\ s^{-1}}) d_{n/nm}^{-1.6} N_{1.45,10-10000} \quad (11)$$

confirms the exponent –1.6 of nanoparticle diameter proposed by Lehtinen *et al*. (2007) and gives an exponent of 1.45 of background particle diameter. Unfortunately, the power-weighted concentration with an exponent of 1.45 cannot be considered a well comprehensible or widely used parameter of the background aerosol and Eq. 11 is not handy when the task is to make quick estimates while browsing the data.

A popular integral measure of atmospheric aerosol number concentration is N_{50-500} (Asmi *et al*. 2011). For this size range, the coefficient a optimized for the reference dataset is 1.45×10^{-6} $\mathrm{cm^3\ s^{-1}}$. The corresponding empiric equation

$$S \approx (1.45 \times 10^{-6}\ \mathrm{cm^3\ s^{-1}}) d_{n/nm}^{-1.6} N_{50-500} \quad (12)$$

is well graspable and convenient in practical applications. However, the accuracy of this approximation is not so good; the GSD is estimated to be about 1.3. The deviation of calculated values from reference results (Eqs. 7 and 8) is illustrated in Fig. 5. Approximation fails when the mean diameter of background particles is out of the range of 50–500 nm. Unfortunately, the incidents of small mean diameter happen mostly during burst events and Eq. 12 cannot be recommended when analyzing new particle formation events.

Sink of singly charged nanoparticles and small ions

Singly charged nanoparticles are often called air ions, while the particles of diameter less than 1.5 nm are small ions and particles of diameter 1.5–7.5 nm are intermediate ions. The coagulation coefficient of small air ions with aerosol particles is called the attachment coefficient. The attachment of air ions to aerosol particles was estimated on basis of fundamental calculations by Fuchs (1963), Hoppel and Frick (1986, 1990), and Stommel and Riebel (2007). The fundamental models lead to sophisticated computational algorithms that are inconvenient when solving practical problems of atmospheric aerosol dynamics. Hoppel and Frick (1986, 1990) published extended tables of attachment coefficients based on capacious computations. Tammet (1991), Tammet and Kulmala (2005) and Tammet *et al*. (2006) proposed a computationally convenient mathematical approximation which can replace the tables during the numerical processing of atmospheric aerosol measurements:

$$\left.\begin{aligned} x &= \frac{qe^2}{2\pi\varepsilon_0 kT\left(d_n + d_h\right)} \\ \beta_q\left(d_n, d_h\right) &= 2\pi kT\left(d_n + d_h\right)\sqrt{B_n^2 + B_h^2} \\ &\times\left(1 - \frac{1}{1 + aq(q-1) + \left(d_n + d_h\right)/b}\right) \\ &\times\frac{x}{e^x - 1} \end{aligned}\right\}. \quad (13)$$

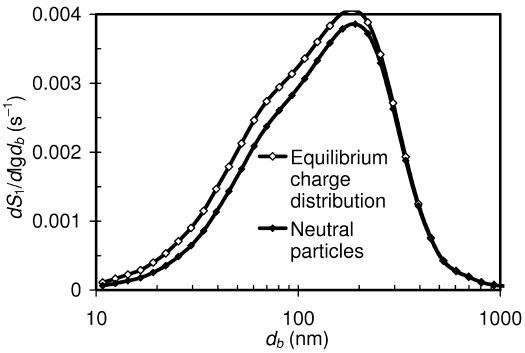

Fig. 6. Mean distribution of small ion sink as a function of the measured diameter of background aerosol particles corresponding to two different assumptions: (1) background aerosol particles have the equilibrium charge distribution, and (2) all background aerosol particles are neutral. Diagrams correspond to small ion mobility of 1.5 cm^2 V^{-1} s^{-1}.

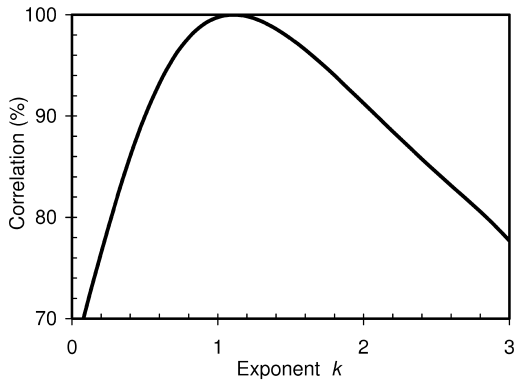

Fig. 7. Correlation between the sink of small ions and the power-weighted concentration of background aerosol particles $N_{k,10-10000}$ depending on the exponent k. The background aerosol is expected to be in equilibrium charging state.

Here x is the dimensionless interaction potential at the contact between the ion and the particle of background aerosol, q is the number of elementary charges on the particle (repelling charge should be presented with a positive and attracting charge with a negative number), e is the elementary charge, ε_o is the electric constant, B_n and B_h are the mechanical mobilities of the air ion and the background aerosol particle, and a and b are the parameters of the mathematical approximation. Parameter values a = 0.4 and b = 25 nm used in present study are optimized for diameters $d_b > 10$ nm. In case of neutral particles $q = 0$ and the term $x/(e^x - 1)$ should be replaced by 1. The mechanical mobility B can be estimated as Z/e, where Z is the electrical mobility of a corresponding singly-charged particle.

Distribution of the sink of singly charged nanoparticles according to the background particle size is characterized with function

$$\frac{dS_1}{dd_b}(d_n, d_b) = \sum_q \beta_q(d_n, d_h)\, n_{bq}(d_b), \quad (14)$$

where n_{bq} is the size distribution of background particles carrying q elementary charges and β_q is the attachment coefficient or coagulation coefficient between a singly charged nanoparticle and a q-charged background particle. Argument of the distribution function of q-charged particles $n_{bq}(d_b)$ is the measured diameter d_b of the particle, but the charge probabilities should be ascertained for corresponding values of natural diameter d_h. The total sink is integral

$$S_1(d_n) = \int_{d_b} \sum_q \beta_q(d_n, d_h)\, n_{bq}(d_b)\, dd_b, \quad (15)$$

where the sum is to be calculated over all negative, zero, and positive values of q. The limits of q depend on the particle size, in the case of d_b = 10 μm, the value of q was varied from –38 to + 38. The effect of background particle charge distribution is significant for smaller aerosol particles up to the diameter of about 400 nm and negligible for large background particles (Fig. 6). Background particles with a diameter around 200 nm have a dominating role in the total sink of small ions just as they dominate the sink of neutral nanoparticles.

The empiric equations were designed following the same method as in the case of sink of neutral nanoparticles. Correlation between the sink of small ions and power-weighted concentrations for the reference set of background aerosol measurements in the full range of 10 nm–10 μm exceeds 99.9% at the exponent of 1.1 (Fig. 7). This is explained by the fact that most of the sink is caused by particles in the size range of about 100–300 nm where attachment is well approximated with Maxwell equation for diffusion deposition and is nearly proportional to the particle diameter. Exponent of 1.1 is close to 1 and satisfactory precision can be achieved as well at exponent 1, in which case the

power-weighted concentration has comprehensible physical interpretation as the diameter length concentration of background aerosol. Diameters of small ions are usually measured with electric mobility spectrometers and the primary information is presented with the measured mobilities Z. Therefore it is reasonable to replace the diameter with corresponding electric mobility Z in the empiric equations. In this case the coefficient of proportionality has dimension of voltage and the optimized empiric equation is

$$S_1 \approx (0.164\ \mathrm{V}) Z \int_{10\ \mathrm{nm}}^{10\ \mu\mathrm{m}} d_\mathrm{b} n_\mathrm{b}(d_\mathrm{b})\, dd_\mathrm{b}. \quad (16)$$

Accuracy of this equation is characterized with GSD = 1.05 or relative standard deviation RSD of about 5% when results of Eq. 16 are compared with estimates according to Eqs. 13 and 15. Equation 16 delivers on average 3% larger values of the sink than an earlier approximation by Tammet (1991), which was based on Smerkalov's mean size distribution of atmospheric aerosols (Smerkalov 1984). The small divergence between two independently derived empiric equations based on different sets of aerosol measurements indicates that the empiric equations may be not very sensitive to specific geographic location.

The diameter length concentration is still not a popular measure of the background aerosol and its values are usually not presented in publications. Thus the practical applications of Eq. 16 are still limited. An alternative empiric equation

$$S_1 \approx (2.6\times10^{-6}\ \mathrm{V\ cm}) Z N_{50-500}. \quad (17)$$

is based on the plain number concentration $N_{50–500}$. Unfortunately, the dispersion between values calculated according to this approximation and the model Eqs. 13 and 15 over the full set of reference measurements is much higher and corresponds to GSD = 1.3.

The probability of having multiple charges on an intermediate ion is negligible and singly charged nanoparticles up to the diameter of 10 nm can be considered in the same way as small ions. The sink of charged nanoparticles on background particles exceeds the sink of neutral particles because the attachment to oppositely charged particles is strongly enhanced and not fully compensated by the reduction of the attachment in case of coinciding polarities. Values of the sink of charged nanoparticles can be calculated according to Eq. 15, considering the actual size and mobility of the particle. Divergence from the distribution of neutral nanoparticle sink is pretty large and dies away only at the diameters above 1000 nm (Fig. 8).

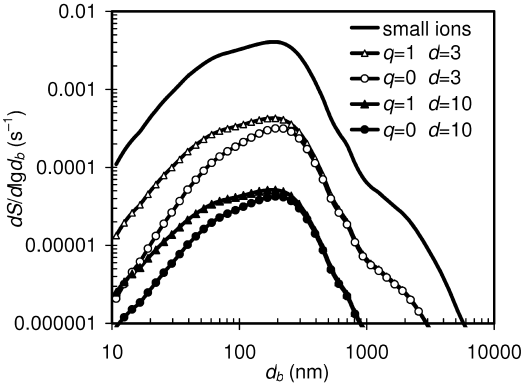

Fig. 8. Distribution of the sink as a function of the diameter of the background aerosol for 5 kinds of nanoparticles: small ions of the mobility of 1.5 cm^2 V^{-1} s^{-1}, and neutral (q = 0) or singly charged (q = 1) nanoparticles of the diameters 3 nm and 10 nm.

An empiric equation for estimating the sink of charged nanoparticles S_1 can be based on an equation derived for the sink of neutral nanoparticles S_0. Dependence of the ratio S_1/S_0 on the nanoparticle diameter in the reference set of background aerosol size distributions is approximated with function

$$S_1(d_\mathrm{n}) \approx \left(1 + \frac{1.5}{\sqrt{d_\mathrm{n/nm}}} - \frac{4}{(d_\mathrm{n/nm}+2)^2}\right) S_0(d_\mathrm{n}). \quad (18)$$

Empiric Eq. 18 and its deviation from fundamental models are illustrated with a diagram in Fig. 9. This equation is neither easily graspable nor convenient for making rough estimates during quick browsing of data but can still serve as a practical tool when analyzing the measurements of intermediate air ions.

Conclusions

An empiric equation may help to make quantita-

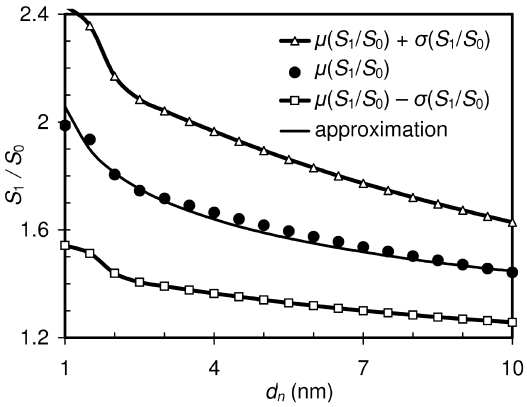

Fig. 9. Dependence of the mean μ and standard deviation σ of the ratio S_1/S_0 of charged and neutral nanoparticle sinks on the nanoparticle diameter in the reference set of background aerosol size distributions. Continuous line near the black circles is drawn according to empiric Eq. 18.

tive relations comprehensible or assist in quick and rough estimation of the coagulation sink according to background aerosol particle concentration and vice versa when browsing limited data. These two goals lead to alternative versions of empiric equations related to the same problem.

A convenient basis for studying the size distribution of atmospheric aerosols is created by transforming the three-year measurement dataset from Hyytiälä, Finland, into a regular table of reference data of 21 682 hourly average distributions.

Two empiric equations are derived to allow estimating the sink of neutral nanoparticles on the preexisting coarse particles of background aerosol. The first equation (Eq. 11) has a low relative standard deviation of 4.5% in the reference set of measurements. It confirms the exponent –1.6 of nanoparticle diameter proposed by Lehtinen *et al*. (2007) and gives an exponent of 1.45 of background particle diameter. The fractional exponent 1.45 is not handy when the task is to make quick estimates while browsing the data. Thus Eq. 11 has only perceptive value. Another equation (Eq. 12) uses plain number concentration $N_{50–500}$ and is convenient in practical applications. However, the accuracy of this approximation is not good; the geometric standard deviation is about 1.3.

Other two empiric equations derived in this study allow the estimation of the sink of small air ions. The first equation (Eq. 16) has a geometric standard deviation of 1.05 through the reference set of measurements. Here the exponent of the background aerosol particle diameter is 1 and the power-weighted concentration has comprehensible physical interpretation as the diameter length concentration of aerosol particles. The values calculated according to this equation differ by 3% from the values calculated according to a similar equation derived by Tammet (1991) on the basis of a distinct size distribution of atmospheric aerosols by Smerkalov (1984). The small difference indicates that the empiric equations may be not very sensitive to specific geographic location. An alternative empiric Eq. 17 uses the plain number concentration $N_{50–500}$ and appears to be more convenient for making quick estimates when browsing the data but has a high geometric standard deviation of about 1.3.

The sink of charged nanoparticles of diameter up to 10 nm or intermediate ions is compared with the sink of neutral particles of the same size. The ratio S_1/S_0 approaches 1 when the diameter of the nanoparticle is increased. Numerical experiments allow approximating the ratio S_1/S_0 with empiric Eq. 18.

Acknowledgements: This research was supported by the Estonian Science Foundation through grant 8342 and the Estonian Research Council Targeted Financing Project SF0180043s08.

References

Adam M., Putaud J.P., Martins dos Santos S., Dell'Acqua A. & Gruening C. 2012. Aerosol hygroscopicity at a regional background site (Ispra) in Northern Italy. *Atmos. Chem. Phys.* 12: 5703–5717.

Asmi A., Wiedensohler A., Laj P., Fjaeraa A.-M., Sellegri K., Birmili W., Weingartner E., Baltensperger U., Zdimal V., Zikova N., Putaud J.-P., Marinoni A., Tunved P., Hansson H.-C., Fiebig M., Kivekäs N., Lihavainen H., Asmi E., Ulevicius V., Aalto P.P., Swietlicki E., Kristensson A., Mihalopoulos N., Kalivitis N., Kalapov I., Kiss G., de Leeuw G., Henzing B., Harrison R.M., Beddows D., O'Dowd C., Jennings S.G., Flentje H., Weinhold K., Meinhardt F., Ries L. & Kulmala M. 2011. Number size distributions and seasonality of submicron particles in Europe 2008–2009. *Atmos. Chem. Phys.* 11: 5505–5538, doi:10.5194/acp-11-5505-2011.

Dahneke B. 1983. Simple kinetic theory of Brownian diffusion in vapors and aerosols. In: Meyer R.E. (ed.), *Theory of dispersed multiphase flow*, Academic Press, New York, pp. 97–133.

Dal Maso M., Kulmala M., Lehtinen K., Mäkelä J.M, Aalto P.P. & O'Dowd, C.D. 2002. Condensation and coagulation sinks and formation of nucleation mode particles in coastal and boreal forest boundary layers. *J. Geophys. Res.* 107: 8097, doi:10.1029/2001JD001053.

Dal Maso M., Kulmala M., Riipinen I., Wagner R., Hussein T., Aalto P.P. & Lehtinen K.E.J. 2005. Formation and growth of fresh atmospheric aerosols: eight years of aerosol size distribution data from SMEAR II, Hyytiälä, Finland. *Boreal Env. Res.* 10: 323–336.

Ehn M., Petäjä T., Aufmhoff H., Aalto P., Hämeri K., Arnold F., Laaksonen A. & Kulmala M. 2007. Hygroscopic properties of ultrafine aerosol particles in the boreal forest: diurnal variation, solubility and the influence of sulfuric acid. *Atmos. Chem. Phys.* 7: 211–222.

Fors E.O., Swietlicki E., Svenningsson B., Kristensson A., Frank G.P. & Sporre M. 2011. Hygroscopic properties of the ambient aerosol in southern Sweden — a two year study. *Atmos. Chem. Phys.* 11: 8343–8361.

Fuchs N.A. 1963. On the stationary charge distribution on aerosol particles in a bipolar ionic atmosphere. *Geofis. pura e appl.* 56: 185–193.

Fuchs N.A. & Sutugin A.G. 1971. High-dispersed aerosols. In: Hidy G.M. & Brock J.R. (eds.), *Topics in current aerosol research*, Pergamon Press, Oxford & New York, pp. 1–60.

Gopalakrishnan R., Thajudeen T. & Hogan C.J. 2011. Collision limited reaction rates for arbitrarily shaped particles across the entire diffusive Knudsen number range. *J. Chem. Phys.* 135: 054302, doi: 10.1063/1.3617251

Hari P. & Kulmala M. 2005. Station for Measuring Ecosystem–Atmosphere Relations (SMEAR II). *Boreal Env. Res.* 10: 315–322.

Hoppel W.A. & Frick G.M. 1986. Ion-attachment coefficients and the steady-state charge distribution on aerosols in a bipolar ion environment. *Aerosol Sci. Technol.* 5: 1–21.

Hoppel W.A. & Frick G.M. 1990. The nonequilibrium character of the aerosol charge distributions produced by neutralizers. *Aerosol Sci. Technol.* 12: 471–496.

Kerminen V.-M. & Kulmala M. 2002. Analytical formulae connecting the "real" and the "apparent" nucleation rate and the nuclei number concentration for atmospheric nucleation events. *J. Aerosol Sci.* 33: 609–622.

Kulmala M. 2003. How particles nucleate and grow. *Science* 302: 1000–1001.

Kulmala M., Vehkamäki H., Petäjä T., Dal Maso M., Lauri A., Kerminen V.-M., Birmili W. & McMurry P.H. 2004. Formation and growth rates of ultrafine atmospheric particles: a review of observations. *J. Aerosol Sci.* 35: 143–176.

Kulmala M., Petäjä T., Nieminen T., Sipilä M., Manninen H.E., Lehtipalo K., Dal Maso M., Aalto P.P., Junninen H., Paasonen P., Riipinen I., Lehtinen K.E.J., Laaksonen A. & Kerminen V.-M. 2012. Measurement of the nucleation of atmospheric aerosol particles. *Nature Protocols* 7: 1651–1667.

Kulmala M., Kontkanen J., Junninen H., Lehtipalo K., Manninen H.E., Nieminen T., Petäjä T., Sipilä M., Schobesberger S., Rantala P., Franchin A., Jokinen T., Järvinen E., Äijälä M., Kangasluoma J., Hakala J., Aalto P.P., Paasonen P., Mikkilä J., Vanhanen J., Aalto J., Hakola H., Makkonen U., Ruuskanen T., Mauldin R.L. 3rd, Duplissy J., Vehkamäki H., Bäck J., Kortelainen A., Riipinen I., Kurtén T., Johnston M.V., Smith J.N., Ehn M., Mentel T.F., Lehtinen K.E., Laaksonen A., Kerminen V.-M. & Worsnop D.R. 2013. Direct observations of atmospheric aerosol nucleation. *Science* 339: 943–946.

Lehtinen K.E.J., Dal Maso M., Kulmala M. & Kerminen V.-M. 2007. Estimating nucleation rates from apparent particle formation rates and vice versa: Revised formulation of the Kerminen-Kulmala equation. *J. Aerosol Sci.* 38: 988–994.

Manninen H.E., Nieminen T., Asmi E., Gagné S., Häkkinen S., Lehtipalo K., Aalto P., Vana M., Mirme A., Mirme S., Hõrrak U., Plass-Dülmer C., Stange G., Kiss G., Hoffer A., Töro N., Moerman M., Henzing B., de Leeuw G., Brinkenberg M., Kouvarakis G.N., Bougiatioti A., Mihalopoulos N., O'Dowd C., Ceburnis D., Arneth A., Svenningsson B., Swietlicki E., Tarozzi L., Decesari S., Facchini M.C., Birmili W., Sonntag A., Wiedensohler A., Boulon J., Sellegri K., Laj P., Gysel M., Bukowiecki N., Weingartner E., Wehrle G., Laaksonen A., Hamed A., Joutsensaari J., Petäjä T., Kerminen V.-M. & Kulmala M. 2010. EUCAARI ion spectrometer measurements at 12 European sites — analysis of new-particle formation events. *Atmos. Chem. Phys.* 10: 7907–7927.

Otto E., Fissan H., Park S.H. & Lee K.W. 1999. The log-normal size distribution theory of Brownian aerosol coagulation for the entire particle size range: part II — analytical solution using Dahneke's coagulation kernel. *J. Aerosol Sci.* 30:17–34.

Smerkalov V.A. [Смеркалов В.А.] 1984. [Mean aerosol size distribution approximation]. *Izv. Akad. Nauk SSSR, Fiz. Atmos. Okeana* 20: 317–321. [In Russian].

Stommel Y.G. & Riebel U. 2007. Comment on the calculation of the steady-state charge distribution on aerosols < 100 nm by three body trapping method in a bipolar ion environment. *Aerosol Sci. Technol.* 41: 840–847.

Tammet H. 1991. Aerosol electrical density: interpretation and principles of measurement. *Rep. Series Aerosol Sci.* 19: 128–133.

Tammet H. 1995. Size and mobility of nanometer particles, clusters and ions. *J. Aerosol Sci.* 26: 459–475.

Tammet H. 2012. The function-updated Millikan model: a tool for nanometer particle size-mobility conversions. *Aerosol Sci. Technol.* 46: 10, i–iv.

Tammet H. & Kulmala M. 2005. Simulation tool for atmospheric aerosol nucleation bursts. *J. Aerosol Sci.* 36: 173–196.

Tammet H., Hõrrak U., Laakso L. & Kulmala M. 2006. Factors of air ion balance in a coniferous forest according to measurements in Hyytiälä, Finland. *Atmos. Chem. Phys.* 6: 3377–3390.

Virkkula A., Backman J., Aalto P.P., Hulkkonen M., Riuttanen L., Nieminen T., Dal Maso M., Sogacheva L. De Leeuw G. & Kulmala M. 2011. Seasonal cycle, size

dependencies, and source analyses of aerosol optical properties at the SMEAR II measurement station in Hyytiälä, Finland. *Atmos. Chem. Phys.* 11: 4445–4468.

Westervelt D.M., Riipinen I., Pierce J.R., Trivitayanurak W. & Adams P.J. 2012. Formation and growth of nucleated particles: observational constraints on cloud condensation nuclei budgets. *Atmos. Chem. Phys. Discuss.* 12: 11765–11822.